Setup of radial-axial ring rolling process: combining the worksheet of stability rules with FE simulation

Guido Berti and **Manuel Monti**
University of Padova, DTG, Stradella San Nicola 3, I-36100 Vicenza (Italy)
guido.berti@unipd.it, manuel.monti@unipd.it

Abstract

The paper discusses the stability rules that make it possible to perform the optimal setup of the radial-axial ring rolling process. To assure the continuous forming of the ring different conditions should be satisfied, some concerning the initial shape of the ring, others relevant to the motion of the mandrel, of the conical rolls and of the main roll. The paper presents firstly the mathematical models relevant to the correlations and the reasonable ranges of the key process variables aimed to assure the stable forming condition for the radial-axial ring rolling process. In the second part, to help the process planner in the determination of an initial feasible setup of radial-axial ring rolling process, the rules have been organized in a worksheet suitable for cylindrical rings. Finally the proposed methodology is applied to different rings where the FE simulation has been set up as determined with the worksheet and using Simufact.Forming 11.01 software.

1. Introduction

Radial-axial ring rolling is a metal-forming process for manufacturing seamless annular forgings that are accurately dimensioned and have circumferential grain flow [1]. This process is characterized by complex coupled thermo-mechanical deformation behaviour which deeply influences the forming quality.

In this process, a heated annular blank, is placed between mandrel and main roll and rests on table plates. The main roll controls the continuous rotation of the ring while the mandrel moving towards the main roll squeezes the ring wall causing the expansion of the ring. Two conical rolls act on a section of ring located at 180° respect to the section deformed by the main roll and the mandrel: they are used for the stabilization of the ring as well as for the ring-height control. The upper conical roll can be moved vertically towards the lower one in order to reduce the ring height. Both conical rolls can be moved horizontally to follow the expansion of the ring. Stabilization and centering of the ring during its deformation is improved by the action of two centering rolls which contact the outer surface of the ring and are controlled by a linkage mechanism. During the

expansion of the ring the cross section is reduced, the circumferential length increases and the stiffness of the ring reduces too; for this reason the speed of the mandrel against the main roll as well as the vertical speed of the upper conical roll should be reduced as the ring expands. A schematic illustration of radial–axial ring rolling mill is shown in Figure 1.

The setup of the process can be effectively operated by FE simulation as shown in [2], but the computational effort required is high. This analysis indicates that, during the radial-axial ring rolling process, the radial deformation and the axial deformation develop at the same time but in different sections of the ring. These two local plastic deformation zones are dynamically changing and cause a non-uniform deformation and temperature distribution which deeply influences the forming quality of the ring. If nonuniform deformation and temperature distributions occur during the radial-axial ring rolling process, it will not only result in different microstructure defects, but also leads to internal cracks of the ring, or even causes the interruption of the process [3]. A trial and error procedure in finding an opportune combination of the different motion laws should be avoided and it is suggested to start with an already feasible setup.

Different conditions should be satisfied in order to assure the continuous forming of the ring, some concerning the initial shape of the ring, others relevant to the motion of the mandrel, of the conical rolls and of the main roll. To help the process planner in the determination of an initial feasible setup of radial-axial ring rolling process the known rules have been organized in a worksheet suitable for cylindrical rings. Starting from the final dimensions of the ring, the geometry of the annular blank is determined and, according to the characteristics of the radial-axial ring rolling mill, the planner can determine: i) the feed speeds for the mandrel and the upper axial roll, ii) the position of axial roll respect to the ring and, iii) the synchronization of the mandrel with the conical rolls. As pointed out by Guo [4] the mandrel and the conical rolls should move at velocities changing with time and therefore the feed speed of the mandrel is varied adopting a linear law and the feed speed of the conical roll is determined according to the rule proposed by Keeton.

In the first part the paper the mathematical relationship adopted are summarized and discussed. In the second part the proposed methodology is applied to different rings (small, medium and large diameter presenting different values of the ratio between the height and the thickness of ring section) where the FE simulation has been set up as determined with the worksheet and using Simufact.Forming 11.01 software.

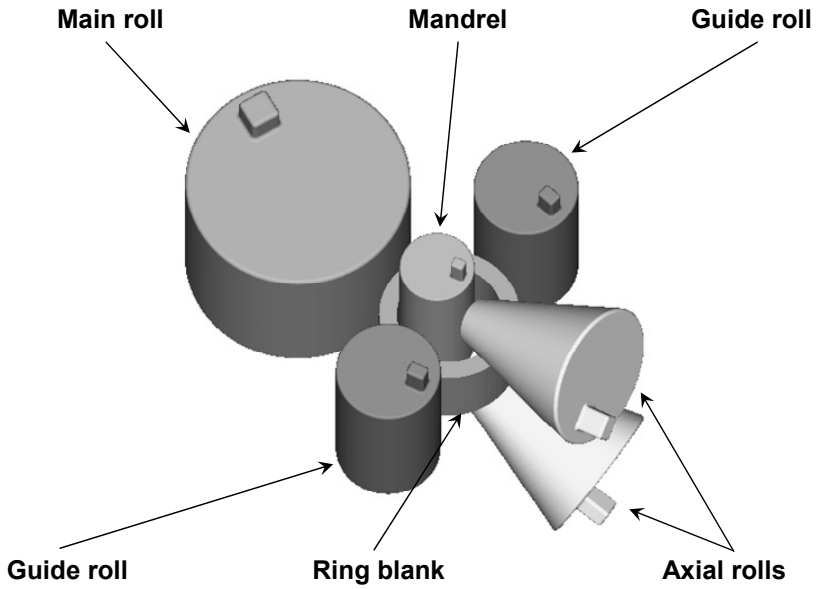

Figure 1: Schematic illustration of radial–axial ring rolling mill.

2. Mathematical modeling of stable forming condition

2.1. Blank size definition

In order to minimize the surface defects (fishtail and folder), Keeton [5] proposed, for the design of the ring blank, the following relationship between the height *h* and the wall thickness *s* of the ring:

$$h^2 - s^2 = const \tag{1}$$

Keeton's method can be used to determine the size of the ring blank. According to eq. (1) we have:

$$h_0^2 - s_0^2 = h_f^2 - s_f^2 \tag{2}$$

and

$$\frac{h_0}{h_f} = \sqrt{1 - \left(\frac{s_f}{h_f}\right)^2 + \left(\frac{s_0}{h_f}\right)^2} \tag{3}$$

where h_0 and s_0 denote the initial height and the initial wall thickness of the ring, and h_f and s_f the final height and the final wall thickness respectively.

According to the principle of volume constancy in plastic deformation we have:

$$\pi\left(D_0^2 - d_0^2\right)h_0 = \pi\left(D^2 - d^2\right)h \tag{4}$$

where D_0 and d_0 are respectively the initial outer and inner diameter of the ring and D and d the instantaneous outer and inner diameter.

According to eqs. (3) and (4) we can obtain:

$$\frac{\left(D_f + d_f\right)}{2\left(d_0 + s_0\right)} = \frac{s_0}{s_f}\sqrt{1 - \left(\frac{s_f}{h_f}\right)^2 + \left(\frac{s_0}{h_f}\right)^2} \tag{5}$$

Rearranging eq. (5) it is possible to obtain the following equation with one unknown quantity s_0.

$$4s_0^6 + ms_0^5 + ns_0^4 + ps_0^3 + qs_0^2 + r = 0 \tag{6}$$

where m, n, p, q, r are equation coefficients, and:

$$\begin{cases} m = 8d_0 \\ n = 4\left(d_0^2 + h_f^2 - s_f^2\right) \\ p = 8d_0\left(h_f^2 - s_f^2\right) \\ q = 4d_0^2\left(h_f^2 - s_f^2\right) \\ r = -\left(D_f + d_f\right)^2 s_f^2 h_f^2 \end{cases} \tag{7}$$

The inner diameter of the ring blank should be generally slightly bigger than that of the mandrel (D_M), generally:

$$1.2D_M \le d_0 \le 1.4D_M \tag{8}$$

This condition makes it possible to reduce the material's scrap during the forming phase of the annular blank. However in order to improve the stability of the radial-axial ring rolling process, it should be necessary to increase the inner diameter of the blank.

Substituting d_0 and the size of the rolled ring into eq. (8), the wall thickness s_0 of the ring can be calculated numerically adopting the algorithm integrated in the worksheet.

Once the wall thickness s_0 of the ring is calculated, it is possible to obtain the initial outer diameter of the ring:

$$D_0 = d_0 + 2s_0 \tag{9}$$

According to eq. (4) it is possible to obtain the initial height of the ring.

$$h_0 = \sqrt{h_f^2 - s_f^2 + s_0^2} \tag{10}$$

2.2. Reasonable ranges of the rotational speeds for main roll

To ensure the stability of the radial-axial ring rolling process, the linear speed of the ring, in the practical process of radial-axial ring rolling, keeps at the range of 400 - 1600 mm/s [6].

Neglecting the relative sliding between the main roll and ring, one obtains:

$$\omega_R R_R = V_{TA} \tag{11}$$

where ω_R is the rotation speed of the main roll, R_R is the radius of the main roll and V_{TA} is the linear speed of the ring. Thus the reasonable range of the rotational speed of the main roll can be described as follows:

$$\frac{400}{R_R} \le \omega_R \le \frac{1600}{R_R} \tag{12}$$

2.3. Withdrawing speed of the axial rolls

The withdrawing speed V_{aw} of the axial rolls can be expressed as follows:

$$V_{aw} = k \cdot V_D \tag{13}$$

where k is the movement factor and V_D is the growth speed of the ring.

Based on the actual radial-axial ring rolling production conditions, the range of k is from 0 to 1 [7]. Figure 2 shows the initial relative position between the upper conical roll and the ring blank and its variation before and after the radial-axial ring rolling process for k=0, K=1/2 and K=1.

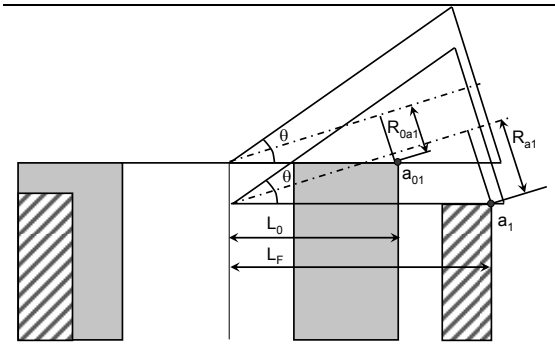	<u>*k=0*</u> the axial rolls are not moving and L is variable (from L_0 to L_F) during the radial-axial ring rolling process. This condition can be adopted for small rings.
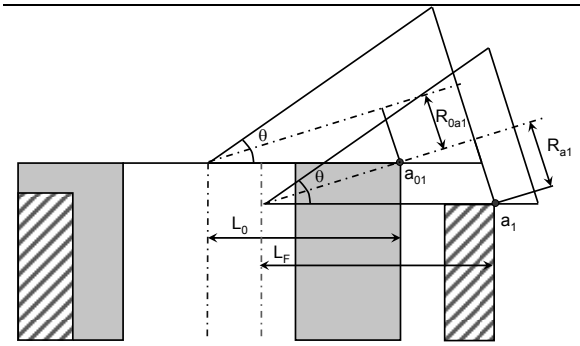	<u>*k=1/2*</u> the vertex of the axial rolls will be placed at the center of the ring for the whole radial-axial ring rolling process and L is variable (from L_0 to L_F). Axial rolls and ring have the same distribution of tangential speeds in the contact zone.

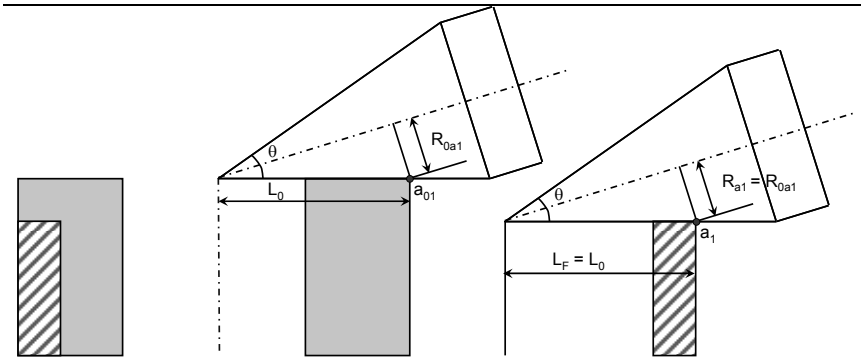

k=1

L is constant during the radial-axial ring rolling process (L_0=L_F). This condition should be adopted for large-scale ring in order to reduce the length of axial rolls.

Figure 2: Position variation of the upper conical roll before and after the radial-axial ring rolling process for different values of the movement factor k.

2.4. Reasonable ranges of the rotational speeds for axial rolls

For the rotational motion of the axial rolls, it shall meet the compatibility condition to ensure stability of the rolling process. Neglecting the relative sliding between the axial rolls and ring, one obtains:

$$\omega_R R_R = \omega_C R_{a1} \tag{14}$$

where ω_C is the rotation speed of the axial rolls and

$$R_{a1} = L\sin\left(\frac{\theta}{2}\right) \tag{15}$$

where L is the distance from the vertex of the axial roll to the contact line between the outside surface of the ring and axial roll and θ is the cone angle of the axial rolls (Figure 2).

Substituting eq. (15) in eq. (14), ω_C can be obtained as follows:

$$\omega_C = \frac{\omega_R R_R}{L\sin\left(\frac{\theta}{2}\right)} \tag{16}$$

L is constant when V_{aw} is equal to V_D *(K=1).* For other values of K, *L* is varying during the process and therefore the rotation speed of the axial rolls is varying from the initial value $[\omega_C]_0$ to the final value $[\omega_C]_F$.

2.5. Reasonable ranges of the feed speed for mandrel

The radial and axial roll passes must meet penetration- and bite-conditions during the radial-axial ring rolling process [8]. The reasonable range of the feed speed for mandrel (V_M) can be expressed as follows:

$$v_{\min,M} \le v_M \le v_{\max,M} \tag{17}$$

where:

$$v_{\min,M} = \frac{\omega_R R_R \Delta s_{\min}}{2\pi R_t} \tag{18}$$

$$v_{\max,M} = \frac{\omega_R R_R \Delta s_{\max}}{2\pi R_t} \tag{19}$$

where $\Delta s_{\min}$ and $\Delta s_{\max}$ are the permitted minimum and maximum values of radial feed amount per revolution and R_t is the instantaneous outer radius of the ring. Eq. (18) and (19) indicate that $v_{\min,M}$ and $v_{\max,M}$ are instantaneous variables. Recent studies focused on how to establish and use steady forming condition for radial-axial ring rolling process, have demonstrated through 3D-FE modeling and simulation of the entire radial-axial ring rolling process, that the feed speed for mandrel (v_M) must decrease gradually to ensure the ring a constant growth velocity [4, 7]. Based on this assumption, the authors propose a decreasing linear function of the feed speed for the mandrel. The initial and final values are respectively $[v_M]_0$ and $[V_M]_F$; their reasonable ranges of variations are defined by the following equations [9].

$$\frac{\omega_R R_R \cdot 6.55 \cdot 10^{-3} \left(R_0 - r_0\right)^2 \left(\frac{1}{R_R} + \frac{1}{R_M} + \frac{1}{R_0} - \frac{1}{r_0}\right)}{2\pi R_0} < \left[v_M\right]_0 < \frac{\omega_R R_R \cdot \frac{2\beta_R^2}{\left(\frac{1}{R_R} + \frac{1}{R_M}\right)^2} \left(\frac{1}{R_R} + \frac{1}{R_M} + \frac{1}{R_0} - \frac{1}{r_0}\right)}{2\pi R_0} \tag{20}$$

$$\frac{\omega_R R_R \cdot 6.55 \cdot 10^{-3} \left(R_F - r_F\right)^2 \left(\frac{1}{R_R} + \frac{1}{R_M} + \frac{1}{R_F} - \frac{1}{r_F}\right)}{2\pi R_F} < \left[V_M\right]_F < \frac{\omega_R R_R \cdot \frac{2\beta_R^2}{\left(\frac{1}{R_R} + \frac{1}{R_M}\right)^2} \left(\frac{1}{R_R} + \frac{1}{R_M} + \frac{1}{R_F} - \frac{1}{r_F}\right)}{2\pi R_F} \tag{21}$$

where R_0 and r_0 are respectively the initial outer and inner radii of the blank, R_F and r_F are respectively the initial outer and inner radii of rolled ring, and β_R is the frictional angle in the radial roll pass.

Once defined $\left[v_M\right]_0$ and $\left[V_M\right]_F$ it is possible to calculate the cycle time for the mandrel ($t_{cycle-M}$) as follows:

$$t_{cycle-M} = \frac{s_0 - s_F}{\frac{\left[v_M\right]_0 + \left[V_M\right]_F}{2}} \tag{22}$$

where s_0 and s_F are the initial and final thickness of the ring. The feed speed and the wall thickness of the ring can be expressed by the following laws:

$$v_M = \left[v_M\right]_0 + \left(\frac{\left[V_M\right]_F - \left[v_M\right]_0}{t_{ciclo-M}}\right) t \tag{23}$$

$$s = s_0 - \left[v_M\right]_0 \cdot t - \left(\frac{\left[V_M\right]_F - \left[v_M\right]_0}{t_{ciclo-M}}\right) \cdot \frac{t^2}{2} \tag{24}$$

2.6. Reasonable range of feed speed for the upper axial roll

The axial roll pass must meet the bite condition. The reasonable range of feed speed for the upper axial roll (v_A) can be expressed as follows:

$$v_{\min,A} \le v_A \le v_{\max,A} \tag{25}$$

$$v_{\min,A} = \frac{\omega_R R_R \Delta h_{\min}}{2\pi R_t} \tag{26}$$

$$v_{\max,A} = \frac{\omega_R R_R \Delta h_{\max}}{2\pi R_t} \tag{27}$$

where $\Delta h_{\min}$ and $\Delta h_{\max}$ are the permitted minimum and maximum values of axial feed amount per revolution and R_t is the instantaneous outer radius of the ring. Eq. (26) and (27) indicate that $v_{\min,A}$ and $v_{\max,A}$ are instantaneous variables. However the feed speed for the upper axial roll should meet the Keeton's condition for the whole radial-axial ring rolling process and, therefore, once the feed speed for the mandrel is defined, the feed speed for the upper axial must satisfy the following relationship:

$$[v_A] = [v_M]\frac{s}{h} \tag{28}$$

The initial and final values are respectively $[v_A]_0$ and $[v_A]_F$. They are defined by the following relationship where $[v_M]_0$ and $[V_M]_F$ are the value of feed speeds of the mandrel defined in the previous section.

$$[v_A]_0 = [v_M]_0 \frac{s_0}{h_0} \tag{29}$$

$$[v_A]_F = [v_M]_F \frac{s_F}{h_F} \tag{30}$$

However it is necessary to verify that the obtained values for $[v_A]_0$ and $[v_A]_F$ meet the bite condition. Their reasonable range of variations is defined by the following equations [9]:

$$\frac{\omega_R R_R \cdot \dfrac{0.0131(h_0)^2}{\left(L_0 - \dfrac{s_0}{2}\right)\tan\left(\dfrac{\theta}{2}\right)}}{2\pi R_0} < [v_A]_0 < \frac{\omega_R R_R \cdot 4\beta_a^2 \left(L_0 - \frac{s_0}{2}\right)\tan\left(\frac{\theta}{2}\right)}{2\pi R_0} \tag{31}$$

and

$$\frac{\omega_R R_R \cdot \dfrac{0.0131(h_F)^2}{\left(L_F - \dfrac{s_F}{2}\right)\tan\left(\dfrac{\theta}{2}\right)}}{2\pi R_F} < [V_A]_F < \frac{\omega_R R_R \cdot 4\beta_a^2 \left(L_F - \frac{s_F}{2}\right)\tan\left(\frac{\theta}{2}\right)}{2\pi R_F} \tag{32}$$

where β_a is the frictional angle in the axial roll pass.

3. The worksheet

To help the process planner in the determination of an initial feasible setup of radial-axial ring rolling process the known rules have been organized in a worksheet suitable for cylindrical rings. Starting from the final dimensions of the ring, the geometry of the annular blank is determined and, according to the characteristics of the radial-axial ring rolling mill, the planner can determine: i) the feed speeds for the mandrel and the upper axial roll, ii) the position of axial roll respect to the ring and, iii) the synchronization of the mandrel with the conical rolls. A snapshot of the worksheet is shown in Figure 3.

template	*grandezze espresse in mm, s, rad*		
Geometria iniziale anello	$400<D_0<3000$	646.417	
	R_0	323.209	**Verificato**
	R_{0max} $(R_0<R_{0max})$	758.288	
	d_{0_min}	300.000	
	d_{0_max} (può essere superato per ottimizzare velocità)	350.000	
	d_0	325.000	
	r_0	162.500	
	h_{0min} - laminatoio	50.000	**Verificato**
	h_0	182.558	
	h_{0max} - laminatoio	600.000	
	s_0	160.709	**Verificato**
	s_{0max} - laminatoio $(S_0<S_{0max})$	595.940	
	s_{0max} - eq. 53 - garantisce Smin<Smax, Tarato $(S_0<S_{0max})$	595.788	
Geometria finale anello	D_f	2900.000	
	R_f	1450.00	
	d_f	2800.000	
	r_f	1400.00	
	h_f	100.000	
	s_f	50.000	
	Δh	82.558	
	Δs	110.709	
Geometria attrezzature	Semi angolo conicità coni $\theta/2$	0.305	
	Raggio Rullo laminatore radiale R_R	375.000	
	Raggio Mandrino R_M	125.000	
	Distanza vertice cono inizio cono laminatore	235.430	
	Lunghezza massima piano cono	595.940	
attrito	μ [0.3-0.4]	0.380	
	β	0.363	

Blank size definition

K=1			
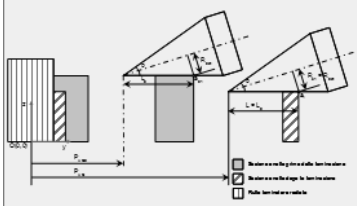	$(L_0-s_0)_{minimo}$	235.430	**Verificato**
	(L_0-s_0)	260.000	
	$(L_0-s_0)_{massimo}$	267.853	
	L_0	420.709	**Verificato**
	$L_{0\ max}$ $(L_0<L_{0\ max})$	831.370	
	P_{VC0}	600.709	
	$(L_0-s_0/2)_{minimo}$ per soddisfare $[V_{min,A}]_0<[V_{max,A}]_0$	91.243	**Verificato**
	$(L_0-s_0/2)$	501.063	
	L_F	420.709	**Verificato**
	$L_{F\ max}$ $(L_F<L_{F\ max})$	831.370	
	$(L_F-s_F/2)_{minimo}$ per soddisfare $[V_{min,A}]_F<[V_{max,A}]_F$	49.981	**Verificato**
	$(L_F-s_F/2)$	395.709	
	(L_F-s_F)	370.709	
‼inserire qui i valori impostati‼	L_0	420.709	
	L_F	420.709	

Movement factor k definition

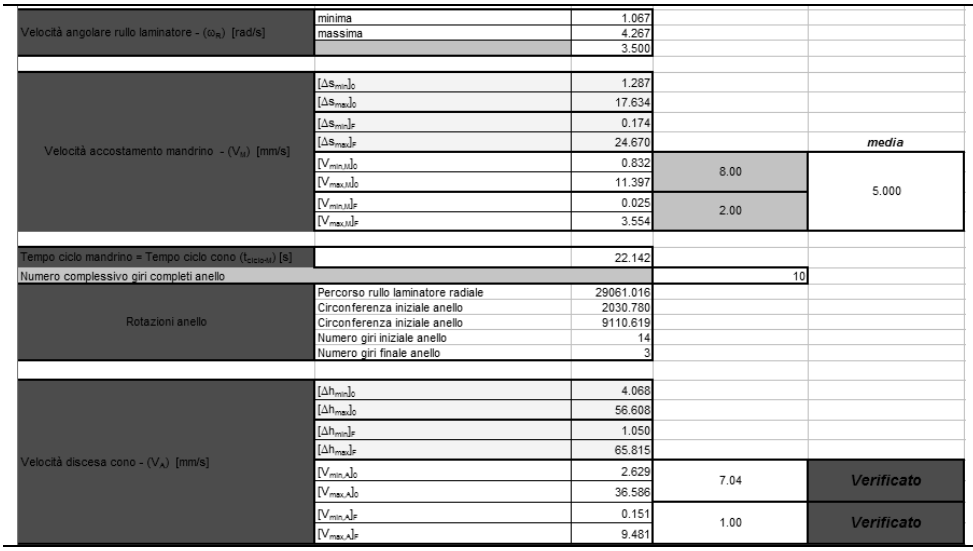

Process parameters range

Figure 3: A snapshot of the worksheet suitable for cylindrical rings that organizes the mathematical models of stable forming condition.

This methodology has been applied to different rings (small, medium and large external diameter), with different ratios between the final thickness and the final height. The numerical simulations plan and relevant blank sizes and ranges of the key process variables is shown in Table 1.

Table 1: Numerical simulations plan.

	Small ring		***Medium ring***		***Large ring***	
Simulation	1	2	3	4	5	6
s_f / h_f	0.69	1.72	0.38	1.50	0.80	1.48
D_f [mm]	809.59	810.00	1100.00	1100.00	2190.00	2180.00
d_f [mm]	645.00	500.00	950.00	800.00	1635.00	1800.00
h_f [mm]	120.00	90.00	200.00	100.00	345.00	128.00
D_0 [mm]	552.92	660.52	607.77	698.09	1345.14	1041.86
d_0 [mm]	325.00	325.00	325.00	325.00	500.00	500.00
h_0 [mm]	143.58	110.53	233.16	149.33	469.66	231.71
k	1	1	1	1	1	1
L_0 [mm]	373.96	407.76	381.39	446.55	754.57	540.93
L_F [mm]	373.96	407.76	381.39	446.55	754.57	540.93
ω_R [rad/s]	3.00	3.00	3.00	3.00	3.00	3.00
$[v_M]_0$ [mm/s]	2.50	2.00	7.50	2.50	5.00	3.00
$[V_M]_F$ [mm/s]	2.00	1.50	5.00	2.00	2.00	1.50
$[v_A]_0$ [mm/s]	1.98	3.04	4.55	3.12	4.50	3.51

$[v_A]_F$ [mm/s]	1.37	2.58	1.88	3.00	1.61	2.23
$[\omega_C]_0$ [rad/s]	10.00	9.18	9.81	8.38	4.96	6.92
$[\omega_C]_F$ [rad/s]	10.00	9.18	9.81	8.38	4.96	6.92

4. Numerical simulations of the radial-axial ring rolling process

The cases described in the previous paragraph and the initial setup as resulted by the utilization of the worksheet have been replicated adopting FE modelization and using Simufact.forming 11.01.

The RAW kinematic module has been used to model the behaviour of centering rolls and Ringmesh has been adopted in discretizing the continuous of the ring geometry. In the model, the material is 42CrMo4 alloy steel which is widely used in the production of large-scale rings for wind power equipment; its physical properties and constitutive model varying with temperature are provided by the material database embedded in Simufact.Forming 11.01. For the different cases the expansion of ring appears to be regular and stable. Small instabilities have been detected in the forming of large rings: these instabilities have been attributed to the coarse mesh adopted to reduce computational time. Figure 4 reports the results in terms of equivalent plastic strain distribution for the different investigated cases showing the initial configuration (on the left) and the final configuration as predicted by the FE simulation (on the right).

Simulation 1	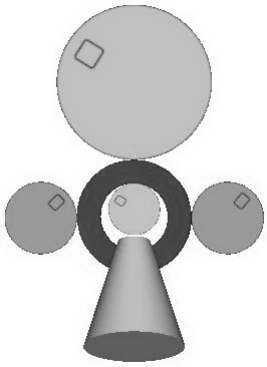	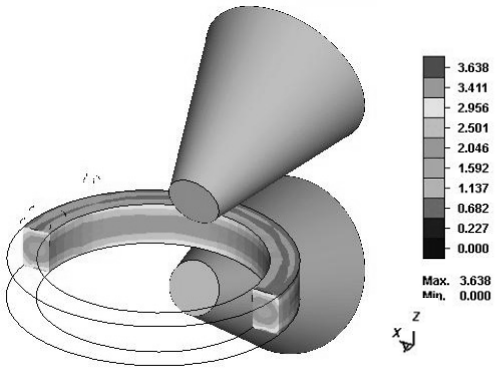

Simulation 2	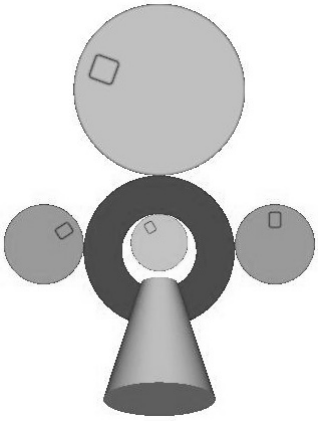	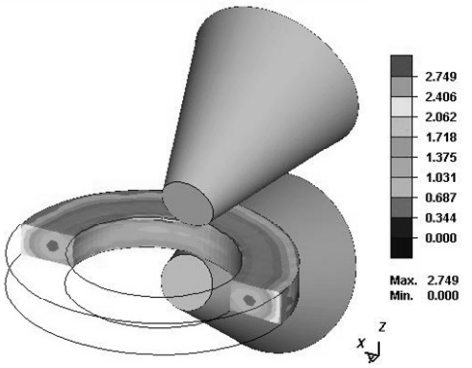
Simulation 3	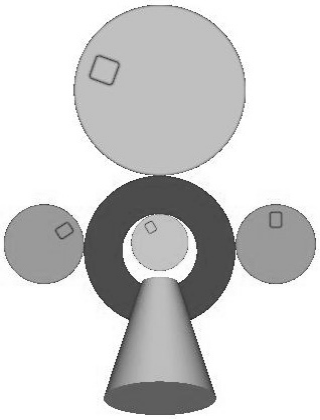	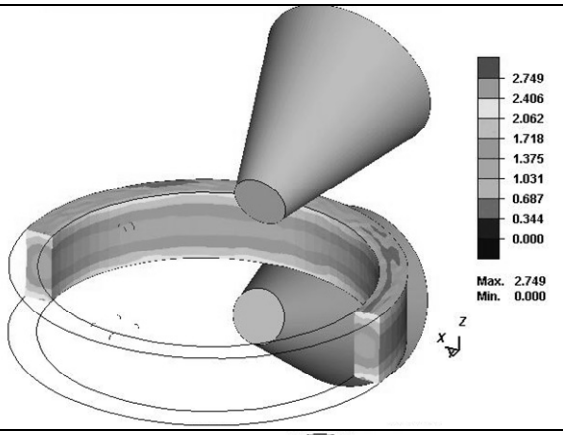
Simulation 4	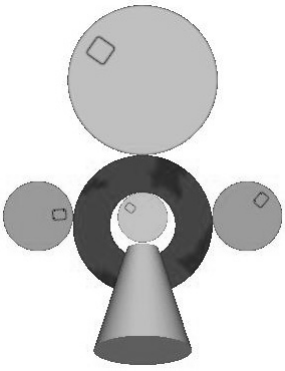	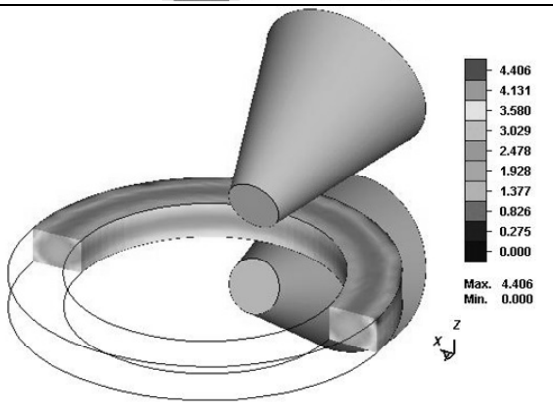

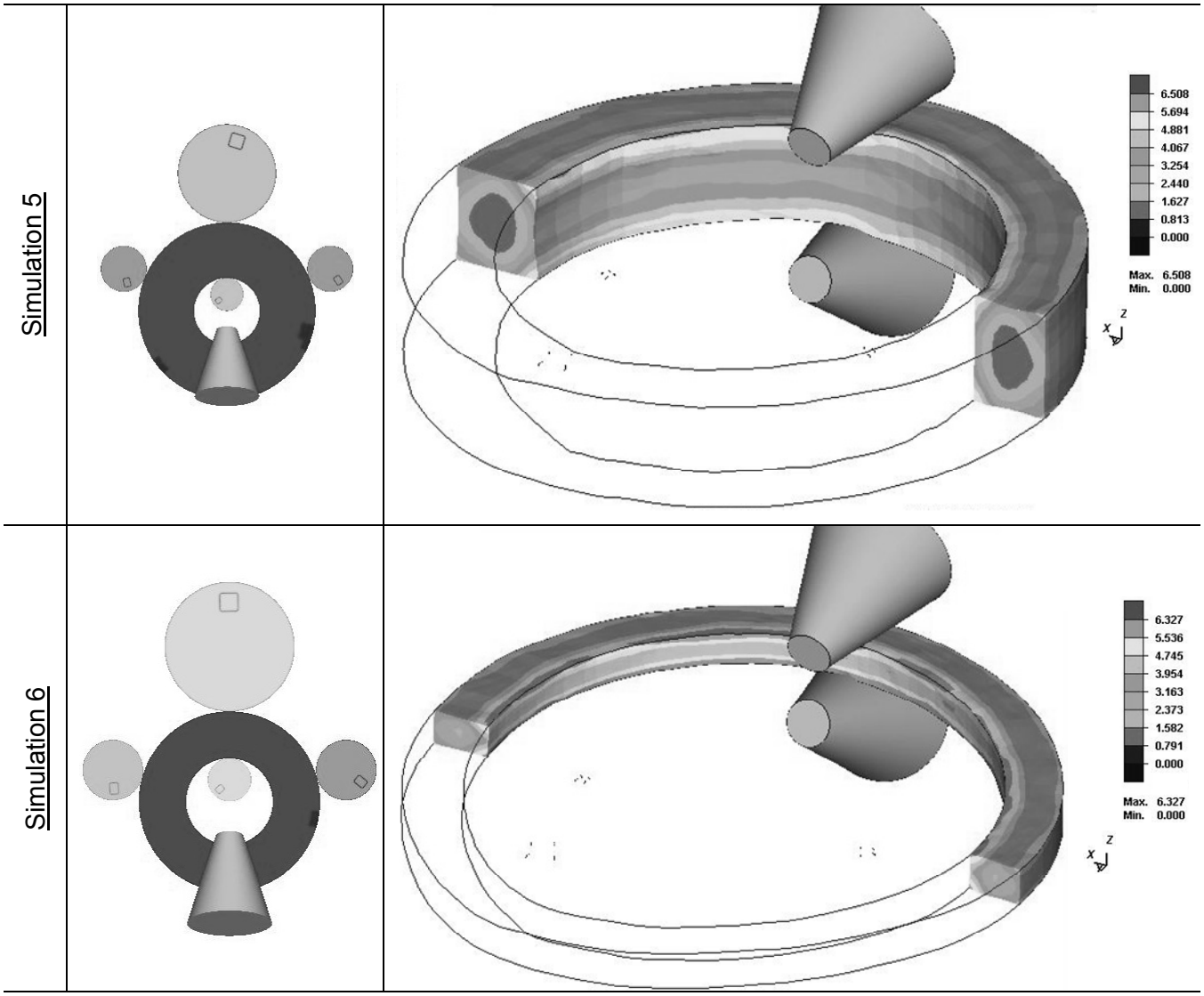

Figure 4: Equivalent plastic strain distribution of radial-axial ring rolling numerical simulations (initial configuration on the left and the final configuration on the right.

5. Conclusions

The study carried out in this paper focuses on how to establish and apply stable forming conditions for radial-axial ring rolling process. The main topic discussed are:

a. The mathematical models relevant to correlations and the reasonable ranges of the key process variables aimed to assure the stable forming condition for the radial-axial ring rolling process.

b. The rules have been organized in a worksheet suitable for cylindrical rings which help the process planner in the determination of an initial feasible setup of radial-axial ring rolling process.
c. The proposed methodology has been applied to different rings (small, medium and large external diameter), with different ratios between the final thickness and the final height. For the different cases the expansion of ring appears to be regular and stable.

References

[1] Eruç, E., Shivpuri, R.: A summary of ring rolling technology-I. Recent trends in machines, processes and production lines. International journal of machine tools & manufacture 32/3 (1992). 379 - 398.

[2] Berti, G., Monti, M.: Design of a flanged ring produced by hot forming using FE analysis. International Journal of Materials Engineering and Technology 7 (2011). 1 - 15.

[3] Zhou, G., Hua, L., Lan, J., Qian, D.S.: FE analysis of coupled thermo-mechanical behaviors in radial-axial rolling of alloy steel large ring. Computational Materials Science 50 (2010). 65 - 76.

[4] Guo, L., Yang, H.: Towards a steady forming condition for radial-axial ring rolling. International Journal of Mechanical Sciences 53 (2011). 286-299.

[5] Keeton, CR.: Ring rolling. Metals handbook: forming and forging. Metals Park, OH: ASM International. 1988.

[6] Zhou, G., Hua, L., Qian, D.S.: 3D coupled thermo-mechanical FE analysis of roll size effects on the radial-axial ring rolling process. Computational Materials Science 50 (2011). 911 - 924.

[7] Zhou, G., Hua, L., Qian, D.S., Shi, D., Li, H.: Effects of axial rolls motions on radial-axial rolling process for large-scale alloy steel ring with 3D coupled thermo-mechanical FEA. Computational Materials Science 59 (2012). 1 - 7.

[8] Lin, H., Zhi, Z.Z.: The extremum parameters in ring rolling. Journal of Materials Processing Technology 69 (1997). 273 - 276.

[9] Berti, G., Monti, M.: Intervalli ammissibili dei parametri di formatura nel processo di laminazione di anelli. Internal report (2012).